

**$k_T$  factorization of exclusive processes**Makiko Nagashima<sup>1</sup> and Hsiang-nan Li<sup>2</sup><sup>1</sup>Department of Physics, Ochanomizu University,  
Bunkyo-ku, Tokyo 112-8610, Japan<sup>2</sup>Institute of Physics, Academia Sinica, Taipei, Taiwan 115, Republic of China<sup>2</sup>Department of Physics, National Cheng-Kung University,  
Tainan, Taiwan 701, Republic of China**abstract**

We prove  $k_T$  factorization theorem in perturbative QCD (PQCD) for exclusive processes by considering  $\pi\gamma^* \rightarrow \gamma(\pi)$  and  $B \rightarrow \gamma(\pi)l\bar{\nu}$ . The relevant form factors are expressed as the convolution of hard amplitudes with two-parton meson wave functions in the impact parameter  $b$  space,  $b$  being conjugate to the parton transverse momenta  $k_T$ . The point is that on-shell valence partons carry longitudinal momenta initially, and acquire  $k_T$  through collinear gluon exchanges. The  $b$ -dependent two-parton wave functions with an appropriate path for the Wilson links are gauge-invariant. The hard amplitudes, defined as the difference between the parton-level diagrams of on-shell external particles and their collinear approximation, are also gauge-invariant. We compare the predictions for two-body nonleptonic  $B$  meson decays derived from  $k_T$  factorization (the PQCD approach) and from collinear factorization (the QCD factorization approach).

**I. INTRODUCTION**

Both collinear and  $k_T$  factorizations are the fundamental tools of perturbative QCD (PQCD), where  $k_T$  denotes parton transverse momenta. For inclusive processes, consider deeply inelastic scattering (DIS) of a hadron, carrying a momentum  $p$ , by a virtual photon, carrying a momentum  $q$ . Collinear factorization [1] and  $k_T$  factorization [2,3,4] apply, when DIS is measured at a large and small Bjorken variable  $x_B \equiv -q^2/(2p \cdot q)$ , respectively. The cross section is written as the convolution of a hard subprocess with a hadron distribution function in a parton momentum fraction  $x$  in the former, and in both  $x$  and  $k_T$  in the latter. When  $x_B$  is small,  $x \geq x_B$  can reach a small value, at which  $k_T$  is of the same order of magnitude as the longitudinal momentum  $xp$ , and not negligible. For exclusive processes, such as hadron form factors, collinear factorization was developed in [5,6,7,8]. The range of a parton momentum fraction  $x$ , contrary to that in the inclusive case, is not experimentally controllable, and must be integrated over between 0 and 1. Hence, the end-point region with a small  $x$  is not avoidable. If there is no end-point singularity developed in a hard amplitude, collinear factorization works. If such a singularity occurs, indicating the breakdown of collinear factorization,  $k_T$  factorization should be employed. Since  $k_T$  factorization theorem was proposed [9,10], there had been wide applications to various processes [11]. However, a rigorous proof is not yet available.

Based on the concepts of collinear and  $k_T$  factorizations, the PQCD [12,13,14,15] and QCD factorization (QCDF) [16] approaches to exclusive  $B$  meson decays have been developed, respectively. As applying collinear factorization to the semileptonic decay  $B \rightarrow \pi\ell\bar{\nu}$  at large recoil, an end-point singularity from  $x \rightarrow 0$  was observed [17]. Some authors then concluded that PQCD is not applicable to these decays even in the heavy quark limit [16]. According to the above explanation, this conclusion is obviously too strong. We would rather conclude that it is collinear factorization which fails, and that exclusive  $B$  meson decays demand  $k_T$  factorization. Retaining the dependence on the parton transverse momentum  $k_T$ , and resumming the resultant double logarithms  $\alpha_s \ln^2 k_T$  into a Sudakov form factor [12], the singularity does not exist. PQCD is then self-consistent and reliable as an expansion in a small coupling constant  $\alpha_s$  [18,19,20].

In this paper we shall prove the factorization theorem with the  $k_T$  dependence included into two-parton meson wave functions and into hard amplitudes. In our previous works we have proposed a simple all-order proof of collinear factorization theorem for the exclusive process  $\pi\gamma^* \rightarrow \gamma(\pi)$  and  $B \rightarrow \gamma(\pi)l\bar{\nu}$  up to the two-parton twist-3 level [21]. The proof of  $k_T$  factorization theorem follows the similar procedures. We stress that it is more convenient to perform  $k_T$  factorization in the impact parameter  $b$  space, in which infrared divergences in radiative corrections can

be extracted from parton-level diagrams explicitly. We shall explain how to construct a gauge-invariant  $b$ -dependent meson wave function defined as a nonlocal matrix element with a special path for the Wilson link. Evaluating this matrix element in perturbation theory, the infrared divergences in the parton-level diagrams are exactly reproduced.

We emphasize that predictions for a physical quantity from  $k_T$  factorization theorem are gauge-invariant, even though three-parton wave functions are not included. The valence partons, carrying only longitudinal momenta, are initially on-shell. They acquire the transverse degrees of freedom through collinear gluon exchanges, before participating hard scattering. Therefore, the parton-level amplitudes are gauge-invariant. A hard amplitude, derived from the parton-level amplitudes with the gauge-invariant and infrared-divergent meson wave function being subtracted, is then gauge-invariant and infrared-finite. At last, we obtain gauge-invariant and infrared-finite predictions by convoluting the hard amplitude with a model wave function, which is determined from nonperturbative methods (such as lattice QCD and QCD sum rules).

## II. FACTORIZATION OF $\pi\gamma^* \rightarrow \gamma(\pi)$

We first prove  $k_T$  factorization theorem for the exclusive process  $\pi\gamma^* \rightarrow \gamma$ . This process, though containing no end-point singularity, is simple and appropriate for a demonstration. The momentum  $P_1$  ( $P_2$ ) of the initial-state pion (final-state photon) is chosen as

$$\begin{aligned} P_1 &= (P_1^+, 0, \mathbf{0}_T) = \frac{Q}{\sqrt{2}}(1, 0, \mathbf{0}_T), \\ P_2 &= (0, P_2^-, \mathbf{0}_T) = \frac{Q}{\sqrt{2}}(0, 1, \mathbf{0}_T). \end{aligned} \quad (1)$$

We concentrate on the kinematic region with large  $Q = \sqrt{-q^2}$ ,  $q = P_2 - P_1$  being the momentum transfer from the virtual photon, in which scattering mechanism is governed by PQCD. The lowest-order diagrams are displayed in Fig. 1. Assume that the on-shell  $u$  and  $\bar{u}$  quarks carry the fractional momenta  $\bar{x}P_1$  and  $xP_1$ , respectively, with  $\bar{x} \equiv 1 - x$ . The reason for considering an arbitrary  $x$  will become clear later. Figure 1(a) gives the parton-level amplitude,

$$\mathcal{G}^{(0)}(x) = -ie^2 \bar{u}(xP_1) \not{\epsilon} \frac{\not{P}_2 - x \not{P}_1}{(P_2 - xP_1)^2} \gamma_\mu u(\bar{x}P_1), \quad (2)$$

where  $\epsilon$  denotes the polarization vector of the outgoing photon. Figure 1(b) leads to the same result.

The factorization in the fermion flow is achieved by inserting the Fierz identity,

$$I_{ij}I_{lk} = \frac{1}{4}I_{ik}I_{lj} + \frac{1}{4}(\gamma^\alpha)_{ik}(\gamma_\alpha)_{lj} + \frac{1}{4}(\gamma^5\gamma^\alpha)_{ik}(\gamma_\alpha\gamma^5)_{lj} + \frac{1}{4}(\gamma^5)_{ik}(\gamma^5)_{lj} + \frac{1}{8}(\gamma^5\sigma^{\alpha\beta})_{ik}(\sigma_{\alpha\beta}\gamma^5)_{lj}, \quad (3)$$

with  $I$  being the identity matrix and  $\sigma_{\alpha\beta} \equiv i[\gamma_\alpha, \gamma_\beta]/2$ . For the momenta chosen in Eq. (1), only the structure  $\gamma^5\gamma^\alpha$  with  $\alpha = +$  contributes to the wave function at leading twist (twist 2). The other structures contribute at higher twists, and the factorization of the corresponding wave functions is similar.

Equation (2) is then factorized into

$$\mathcal{G}^{(0)}(x) = \psi^{(0)}(x)\mathcal{H}^{(0)}(x), \quad (4)$$

where

$$\begin{aligned} \psi^{(0)}(x) &= \frac{1}{4P_1^+} \bar{u}(xP_1)\gamma^5 \not{n}_- u(\bar{x}P_1), \\ \mathcal{H}^{(0)}(x) &= ie^2 \frac{\text{tr}(\not{\epsilon} \not{P}_2 \gamma_\mu \not{P}_1 \gamma^5)}{2xP_1 \cdot P_2}, \end{aligned} \quad (5)$$

with the dimensionless vector  $n_- = (0, 1, \mathbf{0}_T)$  on the light cone, define the lowest-order distribution amplitude and hard amplitude in perturbation theory, respectively. Note that none of  $\mathcal{G}^{(0)}(x)$ ,  $\psi^{(0)}(x)$ , and  $\mathcal{H}^{(0)}(x)$  depends on a transverse momentum in the  $O(\alpha_s^0)$  factorization.

### A. $O(\alpha_s)$ Factorization

Next we consider the  $O(\alpha_s)$  radiative corrections to Fig. 1(a) shown in Figs. 2(a)-2(f), where the gluon carries the loop momentum  $l$ . As stated in [21], there are two types of infrared divergences, soft and collinear, which arise from  $l$  with the components,

$$\begin{aligned} l^+ &\sim l^- \sim l_T \sim \bar{\Lambda}, \\ l^+ &\sim Q, \quad l^- \sim \bar{\Lambda}^2/Q, \quad l_T \sim \bar{\Lambda}, \end{aligned} \quad (6)$$

respectively. Here  $\bar{\Lambda}$ , being of  $O(\Lambda_{\text{QCD}})$ , represents a small scale. Below we work out the factorization of the collinear enhancement from  $l$  parallel to  $P_1$  without integrating out the transverse components  $l_T$ . The prescription is basically similar to that for collinear factorization. The wave function and the hard amplitude then become  $l_T$ -dependent through collinear gluon exchanges.

We derive the  $O(\alpha_s)$   $k_T$  factorization formula, written as the convolution over the momentum fraction  $\xi$  and over the impact parameter  $b$ ,

$$\begin{aligned} \mathcal{G}^{(1)}(x) &= \sum_{i=a}^f \mathcal{G}_i^{(1)}(x), \\ \mathcal{G}_i^{(1)}(x) &= \int d\xi \frac{d^2b}{(2\pi)^2} \phi_i^{(1)}(x, \xi, b) H^{(0)}(\xi, b) + \psi^{(0)}(x) \mathcal{H}_i^{(1)}(x), \end{aligned} \quad (7)$$

The above expression, with the  $O(\alpha_s)$  wave functions  $\phi_i^{(1)}(x, \xi, b)$  and  $H^{(0)}(\xi, b)$  specified, defines the  $O(\alpha_s)$  hard amplitudes  $\mathcal{H}_i^{(1)}(x)$ , which do not contain collinear divergences. It is now obvious why we consider an arbitrary  $x$  for the parton-level diagrams in Figs. 1 and 2: we can obtain the functional form of  $\mathcal{H}_i^{(1)}(x)$  in  $x$ . Equation (7) is a consequence of our assertion that partons acquire transverse degrees of freedom through collinear gluon exchanges:  $\mathcal{H}^{(1)}$ , convoluted with the lowest-order  $l_T$ -independent  $\psi^{(0)}$ , is then identical to that in collinear factorization. As explained later, this consequence is crucial for constructing gauge-invariant hard amplitudes.

Figures 2(a) and 2(c) are self-energy corrections to the external lines. In this case the loop momentum  $l$  does not flow through the hard amplitude. The  $O(\alpha_s)$  wave functions extracted from these two diagrams are the same as in the collinear factorization [21]. We simply quote the results,

$$\phi_a^{(1)}(x, \xi, b) = \frac{-ig^2 C_F}{4P_1^+} \int \frac{d^4l}{(2\pi)^4} \bar{u}(xP_1) \gamma^5 \not{\epsilon}_- \frac{1}{\bar{x} \not{P}_1} \gamma^\nu \frac{\bar{x} \not{P}_1 + \not{l}}{(\bar{x}P_1 + l)^2} \gamma_\nu u(\bar{x}P_1) \frac{1}{l^2} \delta(\xi - x), \quad (8)$$

$$\phi_c^{(1)}(x, \xi, b) = \frac{-ig^2 C_F}{4P_1^+} \int \frac{d^4l}{(2\pi)^4} \bar{u}(xP_1) \gamma^\nu \frac{x \not{P}_1 - \not{l}}{(xP_1 - l)^2} \gamma_\nu \frac{1}{x \not{P}_1} \gamma^5 \not{\epsilon}_- u(\bar{x}P_1) \frac{1}{l^2} \delta(\xi - x). \quad (9)$$

The loop integrand associated with Fig. 2(b) is given by

$$I_b^{(1)} = e^2 g^2 C_F \bar{u}(xP_1) \gamma^\nu \frac{x \not{P}_1 - \not{l}}{(xP_1 - l)^2} \not{\epsilon} \frac{\not{P}_2 - x \not{P}_1 + \not{l}}{(P_2 - xP_1 + l)^2} \gamma_\mu \frac{\bar{x} \not{P}_1 + \not{l}}{(\bar{x}P_1 + l)^2} \gamma_\nu u(\bar{x}P_1) \frac{1}{l^2}. \quad (10)$$

Inserting the Fierz identity, we obtain the wave function,

$$\phi_b^{(1)}(x, \xi, b) = \frac{ig^2 C_F}{4P_1^+} \int \frac{d^4l}{(2\pi)^4} \bar{u}(xP_1) \frac{\gamma^\nu (x \not{P}_1 - \not{l}) \gamma^5 \not{\epsilon}_- (\bar{x} \not{P}_1 + \not{l}) \gamma_\nu}{(xP_1 - l)^2 (\bar{x}P_1 + l)^2 l^2} u(\bar{x}P_1) \delta\left(\xi - x + \frac{l^+}{P_1^+}\right) e^{-i\mathbf{l}_T \cdot \mathbf{b}}. \quad (11)$$

The Fourier transformation introduces the additional factor  $\exp(-i\mathbf{l}_T \cdot \mathbf{b})$  into the wave function  $\phi_b^{(1)}$  compared to the result in collinear factorization [21], since the hard amplitude depends on  $l_T$  in this case.

The integrand associated with the two-particle irreducible diagram in Fig. 2(d) is given by

$$I_d^{(1)} = -e^2 g^2 C_F \bar{u}(xP_1) \not{\epsilon} \frac{\not{P}_2 - x \not{P}_1}{(P_2 - xP_1)^2} \gamma^\nu \frac{\not{P}_2 - x \not{P}_1 + \not{l}}{(P_2 - xP_1 + l)^2} \gamma_\mu \frac{\bar{x} \not{P}_1 + \not{l}}{(\bar{x}P_1 + l)^2} \gamma_\nu u(\bar{x}P_1) \frac{1}{l^2}. \quad (12)$$

To collect the leading contribution,  $\gamma^\nu$  and  $\gamma_\nu$  must be  $\gamma^-$  and  $\gamma_- = \gamma^+$ , respectively. In the collinear region the following approximation holds,

$$(\not{P}_2 - x \not{P}_1) \gamma^\nu (\not{P}_2 - x \not{P}_1 + \not{l}) \approx 2P_2^\nu \not{P}_2, \quad (13)$$

where the  $l^-$  and  $l_T$  terms, being power-suppressed compared to  $P_2^-$ , have been dropped.

The factorization of the collinear enhancement from Figs. 2(d) requires the further approximation for the product of the two internal quark propagators [21],

$$\frac{2P_2^\nu}{(P_2 - xP_1)^2(P_2 - xP_1 + l)^2} \approx \frac{n_-^\nu}{n_- \cdot l} \left[ \frac{1}{(P_2 - xP_1)^2} - \frac{1}{(P_2 - xP_1 + l)^2} \right], \quad (14)$$

where the numerator  $2P_2^\nu$  comes from Eq. (13), and the factor  $n_-^\nu/n_- \cdot l$  is exactly the Feynman rule associated with a Wilson line in collinear factorization. Similarly, we have neglected the power-suppressed terms, such as  $l^2$  and  $xP_1 \cdot l$ . The first (second) term on the right-hand side of Eq. (14) corresponds to the case without (with) the loop momentum  $l$  flowing through the hard amplitude.

The above eikonal approximation also applies to Fig. 2(e). Hence, the extracted  $O(\alpha_s)$  wave functions are written as

$$\begin{aligned} \phi_d^{(1)}(x, \xi, b) &= \frac{-ig^2 C_F}{4P_1^+} \int \frac{d^4 l}{(2\pi)^4} \bar{u}(xP_1) \gamma^5 \not{n}_- \frac{\bar{x} \not{P}_1 + \not{l}}{(\bar{x}P_1 + l)^2} \gamma_\nu u(\bar{x}P_1) \frac{1}{l^2} \frac{n_-^\nu}{n_- \cdot l} \\ &\quad \times \left[ \delta(\xi - x) - \delta\left(\xi - x + \frac{l^+}{P_1^+}\right) e^{-i\mathbf{l}_T \cdot \mathbf{b}} \right], \end{aligned} \quad (15)$$

$$\begin{aligned} \phi_e^{(1)}(x, \xi, b) &= \frac{ig^2 C_F}{4P_1^+} \int \frac{d^4 l}{(2\pi)^4} \bar{u}(xP_1) \gamma_\nu \frac{x \not{P}_1 - \not{l}}{(xP_1 - l)^2} \gamma^5 \not{n}_- u(\bar{x}P_1) \frac{1}{l^2} \frac{n_-^\nu}{n_- \cdot l} \\ &\quad \times \left[ \delta(\xi - x) - \delta\left(\xi - x + \frac{l^+}{P_1^+}\right) e^{-i\mathbf{l}_T \cdot \mathbf{b}} \right], \end{aligned} \quad (16)$$

where the first (second) term in the brackets is associated with the first (second) term on the right-hand side of Eq. (14). Due to the Fourier transformation, the second terms acquire the additional factor  $\exp(-i\mathbf{l}_T \cdot \mathbf{b})$  compared to the results in collinear factorization.

Figure 2(f) does not exhibit a collinear enhancement, since the radiative gluon gives a self-energy correction to the off-shell internal line. Hence, we have  $\phi_f^{(1)}(x, \xi, b) = 0$ . It is easy to observe that the soft divergences cancel among the  $O(\alpha_s)$  radiative corrections. In the soft region of  $l$  we have  $\exp(-i\mathbf{l}_T \cdot \mathbf{b}) \approx 1$  and  $l^+ \approx 0$ , and the two terms in Eqs. (15) and (16) cancel. Similarly, the soft divergences cancel among Figs. 2(a)-2(c). This is the reason we discuss only the factorization of the collinear enhancements.

The above  $O(\alpha_s)$  wave functions can be reproduced by the  $O(\alpha_s)$  terms of the following nonlocal matrix element in the  $b$  space,

$$\phi(x, \xi, b) = i \int \frac{dy^-}{2\pi} e^{-i\xi P_1^+ y^-} \langle 0 | \bar{u}(y) \gamma_5 \not{n}_- P \exp \left[ -ig \int_0^y ds \cdot A(s) \right] u(0) | \bar{u}(xP_1) u(\bar{x}P_1) \rangle, \quad (17)$$

with the coordinate  $y = (0, y^-, \mathbf{b})$ . The path for the Wilson link is composed of three pieces: from 0 to  $\infty$  along the direction of  $n_-$ , from  $\infty$  to  $\infty + \mathbf{b}$ , and from  $\infty + \mathbf{b}$  back to  $y$  along the direction of  $-n_-$  as displayed in Fig. 3. We show that the first piece corresponds to the eikonal line associated with the first terms in Eqs. (15) and (16). Fourier transforming the gauge field  $A(s)$  into  $\tilde{A}(l)$ , we have

$$-ig \int_0^\infty dz \exp[iz(n_- \cdot l + i\epsilon)] n_- \cdot \tilde{A}(l) = g \frac{n_-^\alpha}{n_- \cdot l} \tilde{A}_\alpha(l). \quad (18)$$

The field  $\tilde{A}(l)$ , contracted with other gauge fields, gives the propagator of the gluon attaching the eikonal line. The second piece does not contribute because of the appropriate choice of the small imaginary constant  $+i\epsilon$  in the above expression. The third piece corresponds to the eikonal line associated with the second terms in Eqs. (15) and (16). The additional Fourier factor  $\exp(-i\mathbf{l}_T \cdot \mathbf{b})$  is a consequence of the shift by  $\mathbf{b}$  from the first piece:

$$-ig \int_\infty^{y^-} dz \exp[iz(n_- \cdot l + i\epsilon) - i\mathbf{l}_T \cdot \mathbf{b}] n_- \cdot \tilde{A}(l) = -g \frac{n_-^\alpha}{n_- \cdot l} e^{-i\mathbf{l}_T \cdot \mathbf{b}} e^{il^+ y^-} \tilde{A}_\alpha(l), \quad (19)$$

where the Fourier factor  $\exp(il^+ y^-)$  leads to the function  $\delta(\xi - x + l^+/P_1^+)$ .

At last, for the evaluation of the lowest-order hard amplitude, we neglect only the minus component  $l^-$  in the denominator [see the second term on the right-hand side of Eq. (14)],

$$(P_2 - xP_1 + l)^2 \approx -(2\xi P_1 \cdot P_2 + l_T^2) . \quad (20)$$

Note that in collinear factorization both  $l^-$  and  $l_T$  are dropped. The  $b$ -dependent hard amplitude is then given by,

$$\begin{aligned} H^{(0)}(\xi, b) &= \int d^2 l_T \mathcal{H}^{(0)}(\xi, l_T) \exp(i \mathbf{l}_T \cdot \mathbf{b}) , \\ \mathcal{H}^{(0)}(\xi, l_T) &= i e^2 \frac{\text{tr}(\not{\epsilon} \not{P}_2 \gamma_\mu \not{P}_1 \gamma^5)}{2\xi P_1 \cdot P_2 + l_T^2} . \end{aligned} \quad (21)$$

Equivalently, the above  $\mathcal{H}^{(0)}(\xi, l_T)$  is derived by considering an off-shell  $\bar{u}$  quark, which carries the momentum  $\xi P_1 - \mathbf{l}_T$ , and the leading structure  $\not{P}_1 \gamma_5$  associated with the pion, which is the same as in collinear factorization.

## B. All-order Factorization

In this subsection we present the all-order proof of  $k_T$  factorization theorem for the process  $\pi\gamma^* \rightarrow \gamma$ , and construct the parton-level wave function in Eq. (17). The proof is similar to that for collinear factorization, if it is performed in the impact parameter  $b$  space. It will be observed that collinear factorization is the  $b \rightarrow 0$  limit of  $k_T$  factorization. Therefore, we just highlight the differences, and refer the rest of details to [21]. The idea of the proof is based on induction. The factorization of the  $O(\alpha_s)$  collinear enhancements has been derived in the previous subsection. Consider  $G^{(0)}(x, b)$  and  $G^{(1)}(x, b)$  defined via

$$\mathcal{G}^{(0),(1)}(x) \equiv \mathcal{G}^{(0),(1)}(x, k_T = 0) = \int \frac{d^2 b}{(2\pi)^2} G^{(0),(1)}(x, b) , \quad (22)$$

which indicates that the integration over the variable  $b$  corresponds to an amplitude with  $k_T = 0$  for external particles. The  $O(\alpha_s)$  hard amplitude  $H^{(1)}(\xi, b)$  is defined similarly via  $\mathcal{H}^{(1)}(\xi)$ . We obtain the factorization formula up to  $O(\alpha_s)$ ,

$$G^{(0)}(x, b) + G^{(1)}(x, b) = \int d\xi \left[ \phi^{(0)}(x, \xi, b) + \phi^{(1)}(x, \xi, b) \right] \left[ H^{(0)}(\xi, b) + H^{(1)}(\xi, b) \right] , \quad (23)$$

with  $\phi^{(0)}(x, \xi, b) = \psi^{(0)}(x) \delta(\xi - x)$ . The summation over all the diagrams is understood.

Assume that factorization theorem holds up to  $O(\alpha_s^N)$ ,

$$G^{(j)}(x, b) = \sum_{i=0}^j \int d\xi \phi^{(i)}(x, \xi, b) H^{(j-i)}(\xi, b) , \quad j = 1, \dots, N , \quad (24)$$

where  $\phi^{(i)}(x, \xi, b)$  is given by the  $O(\alpha_s^i)$  terms in the perturbative expansion of Eq. (17).  $H^{(j-i)}(\xi, b)$  stands for the  $O(\alpha_s^{j-i})$  infrared-finite hard amplitude. Equations (23) and (24) approach the expressions in collinear factorization as  $b \rightarrow 0$  as stated above. We shall show that the  $O(\alpha_s^{N+1})$  diagrams  $\mathcal{G}^{(N+1)}$  in the momentum space is written as the convolution of the  $O(\alpha_s^N)$  diagrams  $\mathcal{G}^{(N)}$  with the  $O(\alpha_s)$  wave function by employing the Ward identity,

$$l_\mu G^\mu(l, k_1, k_2, \dots, k_n) = 0 , \quad (25)$$

where  $G^\mu$  represents a physical amplitude with an external gluon carrying the momentum  $l$  and with  $n$  external quarks carrying the momenta  $k_1, k_2, \dots, k_n$ . All these external particles are on the mass shell. It is known that factorization of a QCD process in momentum, spin and color spaces requires summation of many diagrams. With the Ward identity, the diagram summation can be handled in an elegant way.

Look for the gluon in a complete set of  $O(\alpha_s^{N+1})$  diagrams  $\mathcal{G}^{(N+1)}$ , one of whose ends attaches the outer most vertex on the upper  $u$  quark line in the pion. Let  $\alpha$  denote the outer most vertex, and  $\beta$  denote the attachments of the other end of the identified gluon inside the rest of the diagrams. There are two types of collinear configurations associated with this gluon, depending on whether the vertex  $\beta$  is located on an internal line with a momentum along  $P_1$ . The quark spinor adjacent to the vertex  $\alpha$  is  $u(\bar{x}P_1)$ . If  $\beta$  is not located on a collinear line along  $P_1$ , the component  $\gamma^+$  in  $\gamma^\alpha$  and the minus component of the vertex  $\beta$  give the leading contribution. If  $\beta$  is located on a collinear line along  $P_1$ ,  $\beta$  can not be minus, and both  $\alpha$  and  $\beta$  label the transverse components. This configuration is the same as of the self-energy correction to an on-shell particle.

According to the above classification, we decompose the tensor  $g_{\alpha\beta}$  appearing in the propagator of the identified gluon into

$$g_{\alpha\beta} = \frac{n_{-\alpha} l_{\beta}}{n_{-} \cdot l} - \delta_{\alpha\perp} \delta_{\beta\perp} + \left( g_{\alpha\beta} - \frac{n_{-\alpha} l_{\beta}}{n_{-} \cdot l} + \delta_{\alpha\perp} \delta_{\beta\perp} \right). \quad (26)$$

The first term on the right-hand side extracts the first type of collinear enhancements, since the light-like vector  $n_{-\alpha}$  selects the plus component of  $\gamma^{\alpha}$ , and the dominant component  $l_{\beta=-}$  in the collinear region selects the minus component of the vertex  $\beta$ . The components  $l_{\beta=+,\perp}$  do not change the collinear structure, since they are negligible in the numerators compared to the leading terms proportional to  $P_1^+$  and  $P_2^-$ . This can be confirmed by contracting  $l_{\beta}$  to Figs. 2(d) and 2(e), from which Eq. (14) is obtained. The second term extracts the second type of collinear enhancements. The last term does not contribute a collinear enhancement due to the equation of motion for the  $u$  quark. We shall concentrate on the factorization of  $\mathcal{G}_{\parallel}^{(N+1)}$  corresponding to the first term on the right-hand side of Eq. (26), and the factorization associated with the second term can be included simply by following the procedure in [21].

Those diagrams with Figs. 2(a) and 2(b) as the  $O(\alpha_s)$  subdiagrams are excluded from the set of  $\mathcal{G}_{\parallel}^{(N+1)}$  as discussing the first type of collinear configurations, since the identified gluon does not attach a line parallel to  $P_1$ . Consider the physical amplitude, in which the two on-shell quarks and one on-shell gluon carry the momenta  $\bar{\xi}P_1$ ,  $xP_1$  and  $l$ , respectively. Figure 4(a), describing the Ward identity, contains a complete set of contractions of  $l_{\beta}$ , since the second and third diagrams have been added back. The second and third diagrams in Fig. 4(a) lead to

$$l_{\beta} \frac{1}{\bar{\xi} \not{P}_1 - \not{l}} \gamma^{\beta} u(\bar{\xi}P_1) = \frac{1}{\bar{\xi} \not{P}_1 - \not{l}} (l - \bar{\xi} \not{P}_1 + \bar{\xi} \not{P}_1) u(\bar{\xi}P_1) = -u(\bar{\xi}P_1), \quad (27)$$

$$l_{\beta} \bar{u}(xP_1) \gamma^{\beta} \frac{1}{x \not{P}_1 - \not{l}} = -\bar{u}(xP_1), \quad (28)$$

respectively. The terms  $u(\bar{\xi}P_1)$  and  $\bar{u}(xP_1)$  at the ends of the above expressions correspond to the  $O(\alpha_s^N)$  diagrams.

Figure 4(b) shows that the diagrams  $\mathcal{G}_{\parallel}^{(N+1)}$  associated with the first term in Eq. (26) are factorized into the convolution of the parton-level  $O(\alpha_s^N)$  diagrams  $\mathcal{G}^{(N)}$  with the  $O(\alpha_s)$  collinear piece extracted from Fig. 2(d). The double line represents the Wilson line. The first diagram means that the gluon momentum does not flow into  $\mathcal{G}^{(N)}$ , while in the second diagram the gluon momentum does. The similar reasoning applies to the identified gluon, one of whose ends attaches the outer most vertex of the lower  $\bar{u}$  quark line. Substituting Eq. (24) into  $G^{(N)}(\xi, b)$  in the  $b$  space on the right-hand side of Fig. 4(b), and following the procedure in [21], we arrive at

$$G^{(N+1)}(x, b) = \sum_{i=0}^{N+1} \int d\xi \phi^{(i)}(x, \xi, b) H^{(N+1-i)}(\xi, b), \quad (29)$$

with the infrared-finite  $O(\alpha_s^{N+1})$  hard amplitude  $H^{(N+1)}$ . Equation (29) implies that all the collinear enhancements in the process  $\pi\gamma^* \rightarrow \gamma$  can be factorized into the wave function in Eq. (17) order by order.

### C. Gauge Invariance

We now demonstrate the gauge invariance of  $k_T$  factorization theorem. Equation (17) is explicitly gauge-invariant because of the presence of the Wilson link from 0 to  $y$  [3,22]. Below we argue that hard amplitudes in  $k_T$  factorization are also gauge-invariant. Equation (7) approaches the collinear factorization under the approximation,

$$\phi^{(1)}(x, \xi, b) \approx \phi^{(1)}(x, \xi, 0) \equiv \psi^{(1)}(x, \xi), \quad (30)$$

with  $\psi^{(1)}(x, \xi)$  being the distribution amplitude in collinear factorization. The integration of the hard amplitude  $H^{(0)}(\xi, b)$  over  $b$  gives  $\mathcal{H}^{(0)}(\xi, l_T = 0)$ . Hence, we have the collinear factorization formula,

$$\mathcal{G}^{(1)}(x) = \int d\xi \psi^{(1)}(x, \xi) \mathcal{H}^{(0)}(\xi) + \psi^{(0)}(x) \mathcal{H}^{(1)}(x), \quad (31)$$

where the summation over the diagrams has been suppressed. Since  $\mathcal{G}^{(1)}(x)$ ,  $\psi^{(1)}(x, \xi)$ , and  $\mathcal{H}^{(0)}(\xi)$  are gauge-invariant in collinear factorization,  $\mathcal{H}^{(1)}(x)$  is gauge-invariant. From Eq. (7), the gauge invariance of  $\phi^{(1)}(x, \xi, b)$  stated above, together with the gauge invariance of  $\mathcal{G}^{(1)}(x)$  and  $\mathcal{H}^{(1)}(x)$ , then imply the gauge invariance of  $H^{(0)}(\xi, b)$ . Similarly, the  $k_T$  factorization formula of  $O(\alpha_s^2)$ ,

$$\mathcal{G}^{(2)}(x) = \int d\xi \frac{d^2b}{(2\pi)^2} \left[ \phi^{(2)}(x, \xi, b) H^{(0)}(\xi, b) + \phi^{(1)}(x, \xi, b) H^{(1)}(\xi, b) \right] + \psi^{(0)}(x) \mathcal{H}^{(2)}(x) , \quad (32)$$

leads to the gauge invariance of  $H^{(1)}(\xi, b)$ : Both  $\mathcal{G}^{(2)}(x)$  and  $\psi^{(0)}(x) \mathcal{H}^{(2)}(x)$  are gauge-invariant in collinear factorization, and all  $\phi^{(i)}(x, \xi, b)$  are gauge-invariant as explained previously. The gauge invariance of  $H^{(0)}(\xi, b)$  stated above then implies the gauge invariance of  $H^{(1)}(\xi, b)$ . Therefore, the hard amplitudes in  $k_T$  factorization are gauge-invariant at all orders.

Equation (17) plays the role of an infrared regulator for parton-level diagrams. A hard amplitude then corresponds to the regularized parton-level diagrams. After determining the gauge-invariant infrared-finite hard amplitude  $H(x, b)$ , we convolute it with the physical two-parton pion wave function, whose all-order gauge-invariant definition is given by

$$\phi(x, b) = i \int \frac{dy^-}{2\pi} e^{-ixP_1^+ y^-} \langle 0 | \bar{u}(y) \gamma_5 \not{n}_- P \exp \left[ -ig \int_0^y ds \cdot A(s) \right] u(0) | \pi(P_1) \rangle . \quad (33)$$

The valence-quark state  $|\bar{u}(xP_1)u(\bar{x}P_1)\rangle$  has been replaced by the pion state  $|\pi(P_1)\rangle$ , and the pion decay constant  $f_\pi$  has been omitted. The relevant form factor  $F$  for the process  $\pi\gamma^* \rightarrow \gamma$  is then expressed as

$$F = \int dx \frac{d^2b}{(2\pi)^2} \phi(x, b) H(x, b) . \quad (34)$$

We conclude that predictions derived from  $k_T$  factorization theorem are gauge-invariant and infrared-finite.

$k_T$  factorization theorem for the pion form factor involved in the process  $\pi\gamma^* \rightarrow \pi$  can be proved in the same way. The  $O(\alpha_s)$  factorization is similar to the collinear factorization performed in [21]. The only difference is the extra Fourier factor  $\exp(-i\mathbf{l}_T \cdot \mathbf{b})$  associated with the diagrams, in which the loop momentum flows through the hard amplitude. Following the steps in Sec. II A, the eikonal line can be constructed from the diagrams with collinear gluons attaching the hard amplitude and the outgoing pion. The decomposition in Eq. (26) and the whole procedure presented above then apply. That is, the all-order proof is also similar to that of collinear factorization [21]. Compared to the process  $\pi\gamma^* \rightarrow \gamma$ , the structures  $\gamma_5$  and  $\gamma_5\sigma^{\alpha\beta}$  from the Fierz identity contribute, and the corresponding twist-3 pion wave functions appear.

### III. FACTORIZATION OF $B \rightarrow \gamma(\pi)\ell\bar{\nu}$

In this section we prove  $k_T$  factorization theorem for the radiative decay  $B \rightarrow \gamma\ell\bar{\nu}$ , retaining the transverse degrees of freedom of internal particles, and construct the  $B$  meson wave function in the impact parameter  $b$  space. We shall discuss only the  $O(\alpha_s)$  factorization, and demonstrate that the all-order factorization can be proved in a way similar to collinear factorization [21]. The momentum  $P_1$  of the  $B$  meson and the momentum  $P_2$  of the out-going on-shell photon are chosen as

$$P_1 = \frac{M_B}{\sqrt{2}} (1, 1, \mathbf{0}_T) , \quad P_2 = \frac{M_B}{\sqrt{2}} (0, \eta, \mathbf{0}_T) , \quad (35)$$

where the photon energy fraction  $\eta$  is large enough to justify the applicability of PQCD. Assume that the light spectator quark in the  $B$  meson carries the momentum  $k$ . In collinear factorization, only the plus component  $k^+$  is relevant through the inner product  $k \cdot P_2$  [23]. The lowest-order diagrams for the  $B \rightarrow \gamma\ell\bar{\nu}$  decay is displayed in Fig. 1, but with the upper quark (virtual photon) replaced by a  $b$  quark ( $W$  boson).

Bellow we shall concentrate on Fig. 1(a), because Fig. 1(b) is power-suppressed. Figure 1(a) gives the parton-level amplitude,

$$\mathcal{G}^{(0)}(x) = e\bar{u}(k) \not{\epsilon} \frac{\not{P}_2 - \not{k}}{(P_2 - k)^2} \gamma_\mu (1 - \gamma_5) b(P_1 - k) , \quad (36)$$

which does not depend on a transverse momentum. Inserting the Fierz identity in Eq. (3) into to Eq. (36), we obtain Eq. (4) with

$$\begin{aligned} \psi^{(0)}(x) &= \frac{1}{4P_1^+} \bar{u}(k) \gamma_5 \not{n}_- b(P_1 - k) , \\ \mathcal{H}^{(0)}(x) &= -e \frac{\text{tr}[\not{\epsilon} \not{P}_2 \gamma_\mu (1 - \gamma_5) \not{n}_+ \gamma^5] P_1^+}{2xP_1 \cdot P_2} , \\ &= -e \frac{\text{tr}[\not{\epsilon} \not{P}_2 \gamma_\mu (1 - \gamma_5) (\not{n}_+ + \sqrt{2}) \gamma^5]}{2xP_1 \cdot P_2} , \end{aligned} \quad (37)$$

with the dimensionless vector  $n_+ = (1, 0, \mathbf{0}_T)$  on the light cone. We have dropped the higher-power term  $\not{k}$  in the numerator, and the momentum fraction  $x$  is defined by  $x = k^+/P_1^+$ . For the  $B$  meson wave functions, there are two leading-twist components associated with the structures  $\gamma_5 \gamma^\pm$ . For the  $B \rightarrow \gamma l \bar{\nu}$  decay, we choose the structure  $\gamma_5 \gamma^+ = \gamma_5 \not{n}_+$ , since  $\not{\epsilon}$  in Eq. (37) involves  $\gamma_\perp$ , and only the structure  $\gamma^- \gamma_5 = \not{n}_+ \gamma_5$  contributes to the hard amplitude.

Next we consider the  $O(\alpha_s)$  radiative corrections to Fig. 1(a) shown in Figs. 2(a)-2(f). We discuss the factorization of the soft divergence from the loop momentum  $l^\mu \sim (\bar{\Lambda}, \bar{\Lambda}, \bar{\Lambda})$ , where  $\bar{\Lambda}$  can be regarded as the  $B$  meson and  $b$  quark mass difference,  $\bar{\Lambda} = M_B - m_b$ . The dependence of the  $B$  meson wave function on the transverse momentum is generated by soft gluon exchanges. The analysis is similar to that in Sec. II, and we obtain Eq. (7). The factorization of the two-particle reducible diagrams in Fig. 2(a)-(c) is straightforward. Take Fig. 2(b) as an example, which gives the integrand,

$$I_b^{(1)} = ie g^2 C_F \bar{u}(k) \gamma^\nu \frac{\not{k} - \not{l}}{(k-l)^2} \not{\epsilon} \frac{\not{P}_2 - \not{k} + \not{l}}{(P_2 - k + l)^2} \gamma_\mu (1 - \gamma_5) \frac{\not{P}_1 - \not{k} + \not{l} + m_b}{(P_1 - k + l)^2 - m_b^2} \gamma_\nu b(P_1 - k) \frac{1}{l^2}. \quad (38)$$

Employing the eikonal approximation in the heavy-quark limit, we have

$$\frac{\not{P}_1 - \not{k} + \not{l} + m_b}{(P_1 - k + l)^2 - m_b^2} \gamma_\nu b(P_1 - k) \approx \frac{v_\nu}{v \cdot l} b(P_1 - k), \quad (39)$$

with the velocity  $v = P_1/M_B$ . The  $O(\alpha_s)$  wave function extracted from Eq. (38) is then written as

$$\phi_b^{(1)}(x, \xi, b) = \frac{ig^2 C_F}{4P_1^+} \int \frac{d^4 l}{(2\pi)^4} \bar{u}(k) \gamma^\nu \frac{\not{k} - \not{l}}{(k-l)^2} \gamma_5 \not{\epsilon} b(P_1 - k) \frac{v_\nu}{v \cdot l} \delta\left(\xi - x + \frac{l^+}{P_1^+}\right) e^{-il_T \cdot \mathbf{b}}. \quad (40)$$

The loop integrands associated with Figs. 2(d) and 2(e) are given by

$$I_d^{(1)} = -ie g^2 C_F \bar{u}(k) \not{\epsilon} \frac{\not{P}_2 - \not{k}}{(P_2 - k)^2} \gamma^\nu \frac{\not{P}_2 - \not{k} + \not{l}}{(P_2 - k + l)^2} \gamma_\mu (1 - \gamma_5) \frac{\not{P}_1 - \not{k} + \not{l} + m_b}{(P_1 - k + l)^2 - m_b^2} \gamma_\nu b(P_1 - k) \frac{1}{l^2}, \quad (41)$$

$$I_e^{(1)} = ie g^2 C_F \bar{u}(k) \gamma_\nu \frac{\not{k} - \not{l}}{(k-l)^2} \not{\epsilon} \frac{\not{P}_2 - \not{k} + \not{l}}{(P_2 - k + l)^2} \gamma^\nu \frac{\not{P}_2 - \not{k}}{(P_2 - k)^2} \gamma_\mu (1 - \gamma_5) b(P_1 - k) \frac{1}{l^2}, \quad (42)$$

respectively. Neglecting the subleading terms proportional to  $\not{k}$  and  $\not{l}$  in the numerators in comparison with  $\not{P}_2$ , we have the eikonal approximation,

$$\frac{\not{P}_2 - \not{k}}{(P_2 - k)^2} \gamma^\nu \frac{\not{P}_2 - \not{k} + \not{l}}{(P_2 - k + l)^2} \approx \frac{n_-^\nu}{n_- \cdot l} \left[ \frac{1}{(P_2 - k)^2} - \frac{1}{(P_2 - k + l)^2} \right] \not{P}_2, \quad (43)$$

similar to Eq. (14). Inserting the Fierz identity, we extract the  $O(\alpha_s)$  wave functions,

$$\begin{aligned} \phi_d^{(1)}(x, \xi, b) &= \frac{-ig^2 C_F}{4P_1^+} \int \frac{d^4 l}{(2\pi)^4} \bar{u}(xP_1) \gamma_5 \not{\epsilon} b(P_1 - k) \frac{1}{l^2} \frac{n_- \cdot v}{n_- \cdot l v \cdot l} \\ &\quad \times \left[ \delta(\xi - x) - \delta\left(\xi - x + \frac{l^+}{P_1^+}\right) e^{-il_T \cdot \mathbf{b}} \right], \end{aligned} \quad (44)$$

$$\begin{aligned} \phi_e^{(1)}(x, \xi, b) &= \frac{ig^2 C_F}{4P_1^+} \int \frac{d^4 l}{(2\pi)^4} \bar{u}(xP_1) \gamma_\nu \frac{\not{k} - \not{l}}{(k-l)^2} \gamma_5 \not{\epsilon} b(P_1 - k) \frac{1}{l^2} \frac{n_-^\nu}{n_- \cdot l} \\ &\quad \times \left[ \delta(\xi - x) - \delta\left(\xi - x + \frac{l^+}{P_1^+}\right) e^{-il_T \cdot \mathbf{b}} \right]. \end{aligned} \quad (45)$$

The eikonal approximation in Eq. (39) has been applied. Figure 2(f) does not have the soft divergence due to the off-shell internal quark.

It is obvious that the above  $O(\alpha_s)$  parton-level wave functions are similar to those derived in Sec. II: the eikonal line in  $n_-$  is the same as in collinear factorization, and the integrands contain the additional Fourier factor  $\exp(-il_T \cdot \mathbf{b})$ , when the loop momentum flows through the hard amplitude. The decomposition in Eq. (26) and the procedure for the all-order proof presented in Sec. II apply to the  $B \rightarrow \gamma l \bar{\nu}$  decay. We construct a gauge-invariant light-cone  $B$  meson wave function,



$$\phi_+(x, b) = i \int \frac{dy^-}{2\pi} e^{-ixP_1^+ y^-} \langle 0 | \bar{u}(y) \gamma_5 \gamma^+ P \exp \left[ -ig \int_0^y ds \cdot A(s) \right] b_v(0) | B(P_1) \rangle, \quad (46)$$

where  $b_v$  is the rescaled  $b$  quark field characterized by the velocity  $v$ . The lowest-order hard amplitude in the  $b$  space is given by Eq. (21) with

$$\mathcal{H}^{(0)}(\xi, l_T) = -e \frac{\text{tr}[\not{\epsilon} \not{P}_2 \gamma_\mu (1 - \gamma_5) (\not{P}_1 + M_B) (\not{n}_+ / \sqrt{2}) \gamma^5]}{2\xi P_1 \cdot P_2 + l_T^2}, \quad (47)$$

where the momentum fraction  $\xi$  is defined by  $\xi = (k^+ - l^+)/P_1^+$ . The above expression can be derived by considering an off-shell  $\bar{u}$  quark of the momentum  $(\xi P_1^+, 0, -\mathbf{l}_T)$ , and the leading structure  $(\not{P}_1 + M_B)(\not{n}_+ / \sqrt{2})\gamma^5$  associated with the  $B$  meson, which is the same as in collinear factorization.

As emphasized in the Introduction, the semileptonic decay  $B \rightarrow \pi l \bar{\nu}$ , because of the end-point singularities (the failure of collinear factorization), demands  $k_T$  factorization. Its all-order proof is also performed in the same way. Note that for this mode, both the leading-twist  $B$  meson wave functions  $\phi_\pm$ , associated with the structures  $\gamma_5 \gamma^\pm$ , contribute [21].

#### IV. DISCUSSION

We have explained that the range of a parton momentum fraction  $x$  in exclusive processes, contrary to that in inclusive processes, is not experimentally controllable. Hence, the end-point region with a small  $x$  is not avoidable. If a hard amplitude develops an end-point singularity in collinear factorization, implying the importance of the end-point region,  $k_T$  factorization must be employed. Exclusive  $B$  meson decays belong to this category, for which  $k_T$  factorization is a more appropriate tool. We have proved  $k_T$  factorization theorem for the processes  $\pi \gamma^* \rightarrow \gamma(\pi)$  and  $B \rightarrow \gamma(\pi) l \bar{\nu}$  in this paper. The proof performed in the impact parameter  $b$  space indicates that collinear factorization is the  $b \rightarrow 0$  limit of  $k_T$  factorization.

The prescriptions for determining wave functions and hard amplitudes in  $k_T$  factorization theorem are summarized as follows:

- A two-parton  $b$ -dependent wave function is factorized from parton-level diagrams in a way the same as in collinear factorization (for example, under the same eikonal approximation), but the loop integrand is associated with an additional Fourier factor  $\exp(-i\mathbf{l}_T \cdot \mathbf{b})$ , when the loop momentum  $l$  flows through a hard amplitude.
- A  $k_T$ -dependent hard amplitude is obtained in a way the same as in collinear factorization, but considering off-shell external partons, which carry the fractional momenta  $k = xP + \mathbf{k}_T$  ( $k^2 = -k_T^2$ ),  $P$  being the external meson momenta. Then Fourier transform this hard amplitude into the  $b$  space.
- The insertion of the Fierz identity to separate the fermion flow between a wave function and a hard amplitude is the same as in collinear factorization. Take the process  $\pi \gamma^* \rightarrow \pi$  discussed in Sec. II as an example. Up to the twist-3 accuracy for the initial pion, adopt the structures  $\gamma_5 \gamma^+$ ,  $\gamma_5$  and  $\gamma_5 \sigma^{\alpha\beta}$  with  $\alpha, \beta = \pm$ , *i.e.*, without the  $\perp$  components.

Under the above prescriptions, the Wilson link for the  $b$ -dependent wave function is the same as in collinear factorization, but with a shift  $\mathbf{b}$  between the two pieces of paths along the light cone. Both the  $b$ -dependent two-parton meson wave functions and hard amplitudes are gauge-invariant in  $k_T$  factorization, without introducing three-parton wave functions. Therefore, predictions for a physical quantity obtained from  $k_T$  factorization theorem are gauge-invariant. For inclusive processes in small  $x_B$  physics, the gauge invariance of the unintegrated gluon distribution function and of the hard subprocess of reggeized gluons, being also off-shell by  $-k_T^2$ , is ensured in a similar way. The distinction is that the structures of  $\gamma$ -matrices from the Fierz identity are replaced by eikonal vertices, which contain only the longitudinal components [3].

There are more differences between the  $k_T$  factorizations of inclusive and exclusive processes. Inclusive processes involve a single scale, and only single logarithms. Exclusive processes involve two scales (when a valence parton is soft, another is fast), and double logarithms. That is, no rapidity ordering is assumed [24]. Hence, the required resummation techniques are different. The definition of meson wave functions constructed in this work serves as the starting point of  $k_T$  resummation [25, 26, 27]. The resultant Sudakov factor smears the end-point singularity in the semileptonic decay  $B \rightarrow \pi l \bar{\nu}$  by increasing the magnitude of  $k_T$  though infinite many gluon exchanges. The perturbative expansion of decay amplitudes then makes sense. Certainly, this conclusion needs to be justified by evaluating next-to-leading-order corrections in  $\alpha_s$  in  $k_T$  factorization theorem. If higher-order contributions converge quickly enough, the PQCD approach to exclusive  $B$  meson decays will be theoretically solid.

In our next work we shall construct  $k_T$  factorization of two-body nonleptonic  $B$  meson decays. Below we briefly compare the phenomenological consequences for these decays derived from collinear and  $k_T$  factorizations, mentioning only the CP asymmetry in  $B_d^0 \rightarrow \pi^+ \pi^-$  mode. According to the power counting rules of QCDF [16] based on collinear

factorization, the factorizable emission diagram in Fig. 5(a) gives the leading contribution of  $O(\alpha_s^0)$ , since the  $B \rightarrow \pi$  form factor  $F^{B\pi}$  is not calculable. Because Fig. 5(a) is real, the strong phase arises from the factorizable annihilation diagram in Fig. 5(b), being of  $O(\alpha_s m_0/M_B)$ , and from the vertex correction in Fig. 5(c), being of  $O(\alpha_s)$ . For  $m_0/M_B$  slightly smaller than unity, Fig. 5(c) is the leading source of strong phases in collinear factorization (QCDF). In  $k_T$  factorization the power counting rules change. The factorizable emission diagram is calculable and of  $O(\alpha_s)$  as indicated in Fig. 5(d). The factorizable annihilation diagram has the same power counting as for Fig. 5(b). The vertex correction becomes of  $O(\alpha_s^2)$  as shown in Fig. 5(e). Therefore, Fig. 5(b) contributes the leading strong phase in  $k_T$  factorization (PQCD). The strong phases from Fig. 5(b) and 5(c) are opposite in sign, and the former has a large magnitude. This is the reason QCDF prefers a small and positive CP asymmetry  $C_{\pi\pi}$  [28], while PQCD prefers a large and negative  $C_{\pi\pi} \sim -30\%$  [15,29,30]. It is expected that in the near future the two different approaches to exclusive  $B$  meson decays, based on collinear and  $k_T$  factorizations, could be distinguished by experiments [31,32].

We thank J. Kodaira, Y. Koike, T. Morozumi, G. Sterman, and K. Tanaka for useful discussions. The work was supported in part by the National Science Council of R.O.C. under Grant No. NSC-91-2112-M-001-053, by the National Center for Theoretical Sciences of R.O.C., and by Theory Group of KEK, Japan.

- 
- [1] G. Sterman, *An Introduction to Quantum Field Theory*, Cambridge, 1993.
  - [2] S. Catani, M. Ciafaloni and F. Hautmann, Phys. Lett. B **242**, 97 (1990); Nucl. Phys. **B366**, 135 (1991).
  - [3] J.C. Collins and R.K. Ellis, Nucl. Phys. **B360**, 3 (1991).
  - [4] E.M. Levin, M.G. Ryskin, Yu.M. Shabelskii, and A.G. Shuvaev, Sov. J. Nucl. Phys. **53**, 657 (1991).
  - [5] G.P. Lepage and S.J. Brodsky, Phys. Lett. B **87**, 359 (1979); Phys. Rev. D **22**, 2157 (1980).
  - [6] A.V. Efremov and A.V. Radyushkin, Phys. Lett. B **94**, 245 (1980).
  - [7] V.L. Chernyak, A.R. Zhitnitsky, and V.G. Serbo, JETP Lett. **26**, 594 (1977).
  - [8] V.L. Chernyak and A.R. Zhitnitsky, Sov. J. Nucl. Phys. **31**, 544 (1980); Phys. Rep. **112**, 173 (1984).
  - [9] J. Botts and G. Sterman, Nucl. Phys. **B225**, 62 (1989).
  - [10] H-n. Li and G. Sterman, Nucl. Phys. **B381**, 129 (1992).
  - [11] P. Jain *et al.*, Nucl. Phys. **A666**, 75 (2000); H-n. Li, Nucl. Phys. **A684**, 304 (2001) and references therein.
  - [12] H-n. Li and H.L. Yu, Phys. Rev. Lett. **74**, 4388 (1995); Phys. Lett. B **353**, 301 (1995); Phys. Rev. D **53**, 2480 (1996).
  - [13] C.H. Chang and H-n. Li, Phys. Rev. D **55**, 5577 (1997).
  - [14] T.W. Yeh and H-n. Li, Phys. Rev. D **56**, 1615 (1997).
  - [15] Y.Y. Keum, H-n. Li, and A.I. Sanda, Phys. Lett. B **504**, 6 (2001); Phys. Rev. D **63**, 054008 (2001); Y.Y. Keum and H-n. Li, Phys. Rev. **D63**, 074006 (2001).
  - [16] M. Beneke, G. Buchalla, M. Neubert, and C.T. Sachrajda, Phys. Rev. Lett. **83**, 1914 (1999); Nucl. Phys. **B591**, 313 (2000).
  - [17] A. Szczepaniak, E.M. Henley, and S. Brodsky, Phys. Lett. B **243**, 287 (1990).
  - [18] T. Kurimoto, H-n. Li, and A.I. Sanda, Phys. Rev. D **65**, 014007 (2002).
  - [19] H-n. Li, hep-ph/0102013, to appear in Phys. Rev. D.
  - [20] Z.T. Wei and M.Z. Yang, hep-ph/0202018, to appear in Nucl. Phys. B.
  - [21] H-n. Li, Phys. Rev. D **64**, 014019 (2001); M. Nagashima and H-n. Li, hep-ph/0202127.
  - [22] J.C. Collins and D.E. Soper, Nucl. Phys. **B194**, 445 (1982).
  - [23] S. Descotes-Genon and C.T. Sachrajda, hep-ph/0209216; E. Lunghi, D. Pirjol, and D. Wyler, hep-ph/0210091; but see also G.P. Korchemsky, D. Pirjol, and T.M. Yan, Phys. Rev. D **61** (2000) 114510.
  - [24] H-n. Li, Phys. Lett. B **405**, 347 (1997); hep-ph/9703328; H-n. Li and J.L. Lim, Eur. Phys. J. C **10**, 319 (1999).
  - [25] J.C. Collins and D.E. Soper, Nucl. Phys. **B193**, 381 (1981).
  - [26] H-n. Li, Phys. Rev. D **55**, 105 (1997).
  - [27] I.V. Musatov and A.V. Radyushkin, Phys. Rev. D **56**, 2713 (1997).
  - [28] M. Beneke, hep-ph/0207228.
  - [29] C. D. Lü, K. Ukai, and M. Z. Yang, Phys. Rev. D **63**, 074009 (2001).
  - [30] Y.Y. Keum, H-n. Li, and A.I. Sanda, hep-ph/0201103; Y.Y. Keum, hep-ph/0209002; hep-ph/0209208; Y.Y. Keum and A.I. Sanda, hep-ph/0209014.
  - [31] Y. Nir, hep-ph/0208080.
  - [32] J. Rosner, hep-ph/0208243.

**FIG. 1** Lowest-order diagrams for the process  $\pi\gamma^* \rightarrow \gamma$ .

**FIG. 2**  $O(\alpha_s)$  corrections to Fig. 1(a).

**FIG. 3** The path for the Wilson link in a  $b$ -dependent two-parton meson wave function.

**FIG. 4** (a) Ward identity. (b) Factorization of  $\mathcal{G}^{(N+1)}$ .

**FIG. 5** Diagrams contributing to the  $B_d^0 \rightarrow \pi^+ \pi^-$  decay.

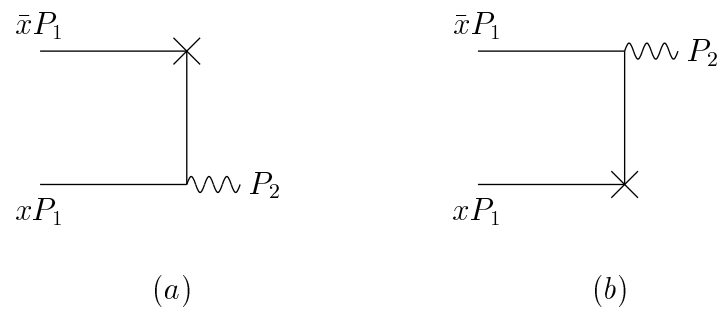
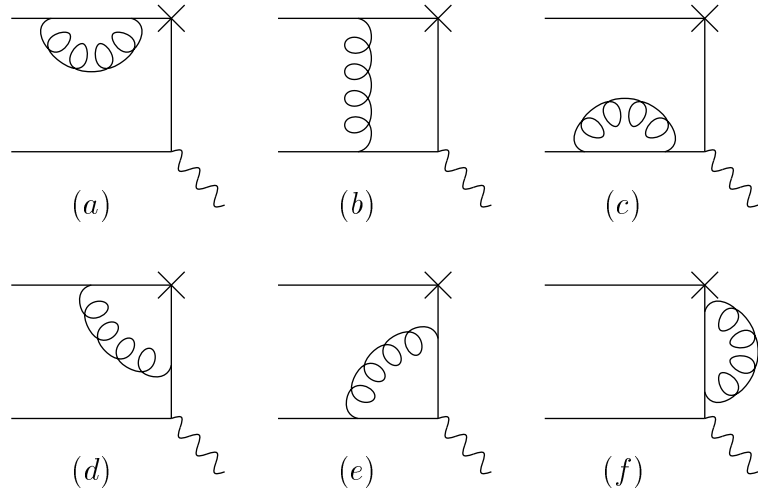
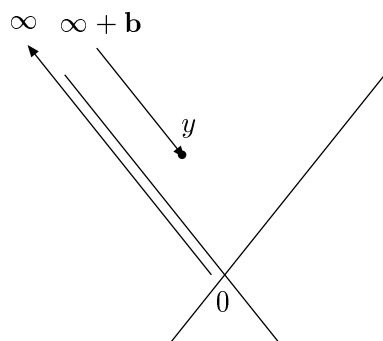


FIG. 1



**FIG. 2**



**FIG. 3**

Diagram (a) shows the sum of three Feynman diagrams. Each diagram consists of two horizontal external lines and a vertical oval blob. In the first diagram, a wavy line with a right-pointing arrow at its end enters the blob from the left; the wavy line is labeled with a subscript  $l$ . In the second diagram, a wavy line enters the blob from the top-left, curves upwards, and ends with an upward-pointing arrow. In the third diagram, a wavy line enters the blob from the top-left, curves downwards, and ends with a downward-pointing arrow. The three diagrams are separated by plus signs, followed by an equals sign and a zero.

(a)

Diagram (b) shows an equation between Feynman diagrams. On the left is a diagram with two horizontal external lines and a vertical oval blob. A wavy line enters the blob from the left, and its end is marked with two parallel horizontal lines. This is equal to a large square bracket containing the sum of two diagrams. The first diagram in the bracket has a wavy line ending in two parallel vertical lines. The second diagram in the bracket has a wavy line ending in two parallel horizontal lines. To the right of the bracket is a tensor product symbol  $\otimes$  followed by a diagram consisting of a vertical oval blob labeled  $\alpha_s^N$  between two horizontal external lines.

(b)

**FIG. 4**

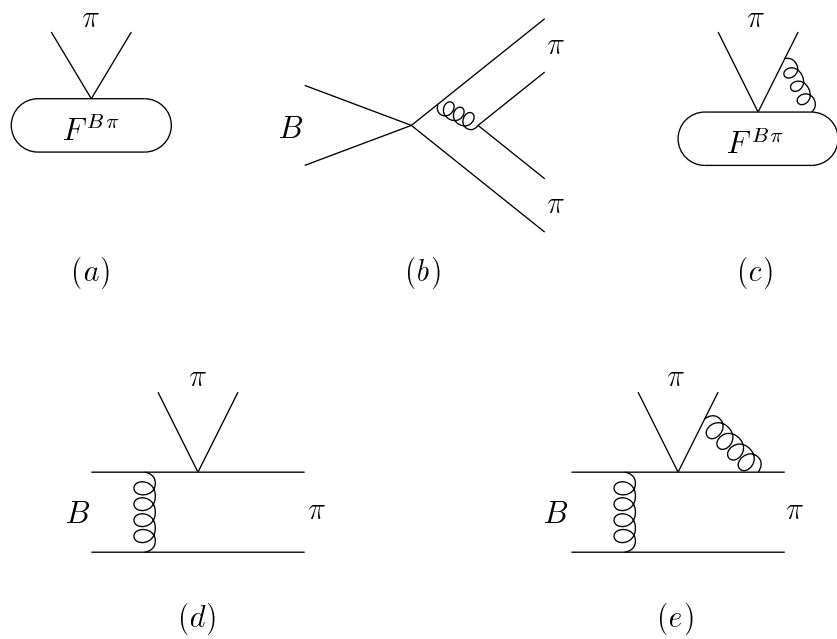


FIG. 5